

Forced motion of a probe particle near the colloidal glass transition

P. Habdas*, D. Schaar, Andrew C. Levitt†, and Eric R. Weeks‡
Physics Department, Emory University, Atlanta, GA 30322

(Dated: May 22, 2019)

We use confocal microscopy to study the motion of a magnetic bead in a dense colloidal suspension, near the colloidal glass transition volume fraction ϕ_g . For dense liquid-like samples near ϕ_g , the magnetic bead remains motionless below a threshold force. Above this force, the bead moves with a fluctuating velocity. The relationship between force and velocity becomes increasingly nonlinear as ϕ_g is approached. The threshold force and nonlinear drag force vary strongly with the volume fraction, while the velocity fluctuations do not change near the transition.

Near the glass transition, molecular motion is greatly slowed, yet this motion is difficult to directly observe and the character of the molecular slowing is hard to determine [1]. Thus, colloidal suspensions of micrometer-sized spheres are a useful model system for investigating the nature of the glass transition, as they can be directly observed using optical microscopy [2, 3, 4, 5]. As the volume fraction of a colloidal suspension is increased, particle motion becomes restricted due to the confining effect of the other particles [4]. For hard spheres above the glass transition volume fraction $\phi_g \sim 0.58$, the particles' diffusion constant becomes zero, and the macroscopic viscosity increases dramatically [6, 7]. Past experiments [2, 3, 4, 5] found that the particle motion in non-driven systems is both spatially heterogeneous and temporally intermittent. However, they did not examine nonequilibrium, driven motion such as that probed by rheology [6, 7].

In this Letter, we study experimentally the motion of a magnetic bead pulled through a dense colloidal suspension. As the colloidal glass transition is approached the motion of the magnetic bead becomes complex. Below a threshold force, the magnetic bead does not move. When the external force is above this threshold, the magnetic bead moves with a fluctuating velocity. Closer to ϕ_g , the threshold force rises, and the velocity-force relationship becomes increasingly nonlinear. Our measurements reveal dramatic changes in the drag force acting on the magnetic bead as the glass transition is approached, indicating a new way to characterize the glass transition.

The colloidal suspensions are made of poly(methylmethacrylate) particles, sterically stabilized by a thin layer of poly-12-hydroxystearic acid [3]. The particles have a radius $a = 1.10 \mu\text{m}$, a polydispersity of $\sim 5\%$, and were dyed with rhodamine. The particles are slightly charged, shifting the phase transition boundaries from those of hard spheres: the freezing transition occurs at $\phi_f \approx 0.38$, the melting transition at $\phi_m \approx 0.42$, and the glass transition at $\phi_g \approx 0.58$. These particles are suspended in a mixture of cyclohexylbromide/*cis*- and *trans*- decalin which nearly matches both the density and the index of refraction of the colloidal particles. We add a small quantity of superparamagnetic beads (Dynal Biotech Inc.) with a radius of $2.25 \mu\text{m}$. Before

beginning experiments, we stir the sample with an air bubble to break up any pre-existing crystalline regions, then wait 20 minutes before taking data.

With a confocal microscope, we rapidly acquire images of area $80 \mu\text{m} \times 80 \mu\text{m}$, containing several hundred particles. The magnetic beads are not fluorescent and thus appear black on the background of dyed colloidal particles. To exert a force on these beads, a Neodymium magnet is mounted on a micrometer held just above the sample. The force is calibrated by determining the velocity of the magnetic beads in glycerol for a given magnet position, and inferring the drag force from Stokes' Law ($F = 6\pi\eta av$, where F is the drag force, η is the viscosity, a is the bead radius, and v is the observed velocity). The imperfect reproducibility of the magnet position causes a 5% uncertainty of the force. Additionally, the beads are not completely monodisperse in their magnetic properties, and our calibration finds the variability in the effective magnetic force to be less than 10%. We study isolated magnetic beads at least $35 \mu\text{m}$ from the sample chamber boundary and from other magnetic beads.

We study the motion of the magnetic beads for a range of forces. Within each image, we locate the center of the magnetic bead with an accuracy of $0.5 \mu\text{m}$ [8]. To show the behavior of the magnetic bead, we plot the average magnetic bead velocity against the applied force on a log-log plot in Fig. 1 for a range of volume fractions. For a dilute system ($\phi=29\%$, asterisks) the data fall on a line with a slope of 1, indicating that the velocity is linearly proportional to the applied force and Stokes' law applies. Due to the nonzero volume fraction, the effective viscosity is modified from that of the solvent ($\eta_0 = 2.25 \text{ mPa}\cdot\text{s}$) to the larger value of $\eta = 6 \pm 1 \text{ mPa}\cdot\text{s}$, in reasonable agreement with past macroscopic measurements in a hard sphere system [7]. Such behavior is expected for low volume fractions, since the moving magnetic bead encounters only a few colloidal particles in its way, and the Reynolds number for the fastest velocity of the magnetic bead is quite small ($Re \approx 2 \times 10^{-6}$).

At higher volume fractions, collisions between the magnetic bead and the colloidal particles become more important (Fig. 1). For data at large forces, the average velocity grows as a power law with force, $\bar{v} \sim F^\alpha$, with

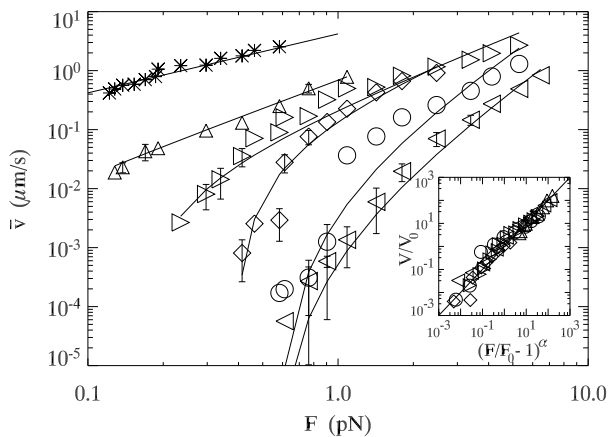


FIG. 1: Velocity of the magnetic bead in the direction of the motion as a function of force acting on the magnetic bead for the volume fractions: 0.29 (*), 0.45 (\triangle), 0.50 (\diamond), 0.53 (\circ), 0.55 (∇). Solid lines are fits to the data obtained using Eq. (1). The uncertainty of F due to the imprecise magnet positioning is not more than 5% and is smaller than the symbol size. Each data set is taken for a single magnetic particle and thus the magnetic particle variability may shift curves relative to each other but does not influence the shape of a curve for a given volume fraction. Where present, the vertical error bars are standard deviations from multiple velocity measurements at the same force. The velocity error due to the uncertainty in the bead position is 5%, smaller than the symbol size. The inset shows the scaling of \bar{v} and F by the fitting parameters.

exponent α between 1.5 and 3. From left to right the curves are increasing in volume fraction, and the slope at the highest forces for each curve increases nearly monotonically, reflecting the approach of the glass transition. For extremely low forces, the magnetic bead does not move more than our resolution limit within four hours, with the observation time limited by the onset of crystallization of the sample; in other words, the velocity is smaller than $4 \cdot 10^{-5} \mu\text{m/s}$. Since the colloidal particles are moving due to Brownian motion one would expect rearrangements to “allow” for the magnetic bead to move, even if this motion would be primarily random with a small bias from the external force.

To determine how the velocity/force relationship changes as the volume fraction is increased, we fit the data to the following equation:

$$\begin{aligned} \bar{v} &= v_0 \cdot \left(\frac{F}{F_0} - 1\right)^\alpha, & F > F_0 \\ &= 0, & F \leq F_0 \end{aligned} \quad (1)$$

where F_0 is a threshold force and α is the exponent characterizing the growth of the velocity at large forces. The use of F_0 in the equation is reasonable, given that the magnetic bead is essentially motionless below a threshold force. v_0 is the velocity the magnetic bead would have if the applied force F was equal to $2F_0$. The solid lines in Fig. 1 are the results of fitting the data with Eq. (1),

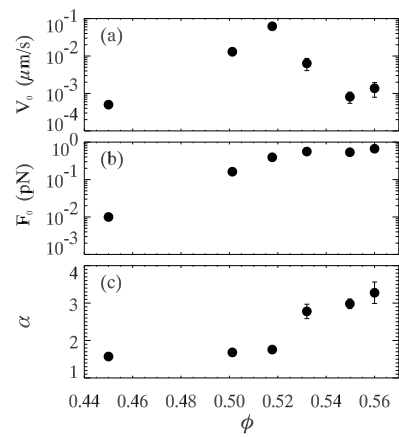


FIG. 2: Fitting parameters as a function of volume fraction: (a) v_0 , (b) threshold force F_0 , and (c) power exponent α . The error bars are due to the uncertainties in measuring the forces and velocities that the model is fit to; where not shown, the errors are smaller than the symbol size.

with the exception of the $\phi = 29\%$ data (asterisks) where Stokes’ Law applies. This model describes the data fairly well for the range of volume fractions studied and captures the rich behavior of the velocity/force relationship.

As the colloidal glass transition is approached the system becomes more viscous, and this is reflected in the changing fit parameters from Eq. (1). This is seen in Fig. 2 which plots the fitting parameters as a function of the volume fraction ϕ . For low volume fractions, the three parameters v_0 , F_0 , and α are all small. This matches the expectation from Stokes’ Law: for $\phi \rightarrow 0$, we expect $F_0 \rightarrow 0$, $v_0 \rightarrow 0$, and $\alpha \rightarrow 1$.

The fit parameters change as the volume fraction $\phi \rightarrow \phi_g$. v_0 initially grows with increasing ϕ and then drops [Fig. 2(a)]. The initial increase presumably reflects the change from the $v_0 \rightarrow 0$ limit at low volume fractions. The decrease as the glass transition is approached then is due to the sharply increasing effective viscosity acting on the magnetic bead. The threshold force F_0 grows as ϕ increases, although it seems to reach a plateau value for large ϕ . We expect that at ϕ_g the threshold force will be finite, both from our data, and also as it seems more likely that F_0 diverges at $\phi_{\text{RCP}} \approx 0.64$, the random close-packing volume fraction [7]. The exponent α changes dramatically as the glass transition is approached, as seen in Fig. 2(c), where it rises above 3 near ϕ_g . Our results are in contrast to Ref. [9]. This may be due to the much different particle interactions in the simulation of unscreened point charges as compared to our colloidal experiment. In our experiments, it is unclear if α diverges at ϕ_g or continues to grow as ϕ_{RCP} is approached. Experiments at $\phi > \phi_g$ are difficult to interpret due to the aging of the sample [10]: for a given force the magnetic bead response depends on the age of the sample.

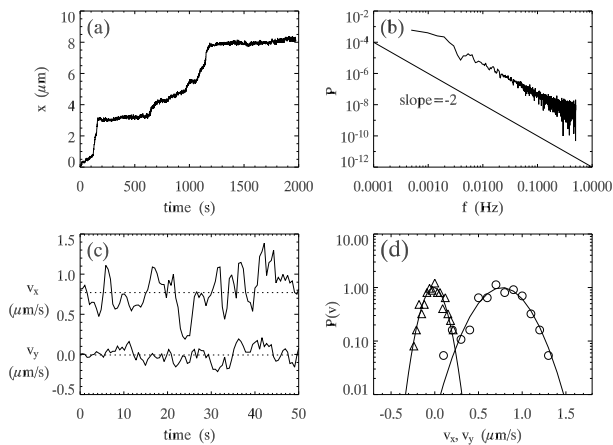


FIG. 3: (a) The position of the magnetic bead in the direction of the motion as a function of time, $F = 0.58pN$, $\phi=52\%$, $\bar{v} = 0.0041\mu\text{m/s}$. (b) The power spectrum of the magnetic bead displacement. The solid line is a guide to the eye and has a slope of -2. The data are the same as (a). (c) The instantaneous velocity in the direction of motion v_x and perpendicular to the motion v_y as a function of time. The velocities are calculated from the displacement data using $\Delta t = 3.2$ s. The dashed lines denote the average velocities $\bar{v}_x = 0.80 \mu\text{m/s}$ and $\bar{v}_y = 0.01 \mu\text{m/s}$. For these data, $\phi=55\%$ and $F=6.46$ pN. (d) The probability distribution of the instantaneous velocities v_x (o) and v_y (Δ). The solid lines denote a Gaussian fit. The data are the same as (c).

Near the glass transition, the motion of the magnetic bead is not smooth, as is seen by a typical plot of its position as a function of time [Fig. 3(a)]. There are both periods of nearly no motion and rapid motion. While the largest “jumps” are roughly the diameter of the surrounding colloidal particles ($2a \sim 2 \mu\text{m}$), at other times the magnetic bead takes much smaller steps. To try to identify a characteristic time scale for these motions, we compute the power spectrum of the position of the magnetic bead, shown in Fig. 3(b). The spectrum has no apparent peaks, but instead decreases steadily, with the high-frequency tail decaying as f^{-2} , as indicated by the straight line. The f^{-2} decay is presumably due to the local random position fluctuations of the magnetic bead due to its Brownian motion. At low frequencies, the lack of a prominent peak in the power spectrum suggests that there is no characteristic time scale for the motion. If there was a peak f_0 , it could be interpreted as a length scale by $l_0 = \bar{v}/f_0$; lacking a clear f_0 shows that there is no characteristic length scale for the motion. This is surprising, given that there are several obvious length scales present, such as the colloidal particle radius a and the magnetic bead radius a_{MB} . (For the data shown in Fig. 3(a,b) these would correspond to $f_a = 0.0039$ Hz and $f_{\text{MB}} = 0.0018$ Hz.) Possibly, we do not have sufficiently long trajectories to get a clean Fourier transform; the duration of our experiments is limited by crystalliza-

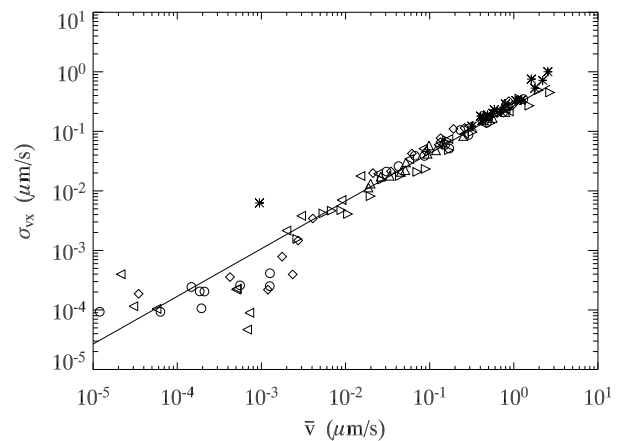


FIG. 4: The standard deviation of the instantaneous distribution of v_x , (σ_{v_x}) as a function of \bar{v} . The solid line is a fit to the data and has a slope of 0.80. The different symbols are volume fractions which are the same as Fig. 1.

tion. Power spectra for different velocities and different volume fractions are similarly featureless.

Given the lack of a characteristic time scale in our experiment, we arbitrarily choose $\Delta t = a_{\text{MB}}/\bar{v}$ as a time scale and define the instantaneous velocity as $\vec{v}(t) = [\vec{r}(t + \Delta t) - \vec{r}(t)]/\Delta t$. The results that follow are not sensitive to this choice (and in particular do not change using a rather than a_{MB}). The instantaneous velocity fluctuations are shown in Fig. 3(c). The magnetic bead velocity has much larger fluctuations along the direction of motion [v_x , top trace in Fig. 3(c)], while fluctuations in the transverse direction are smaller but still noticeable. The distributions of v_x and v_y , shown on Fig. 3(d), are Gaussian (solid fit lines). The velocity fluctuations reflect the fact that the magnetic bead is of similar size to the colloidal particles: its motion is sensitive to colloidal particle configurations, and sometimes to move forward it must also move to the side. The fluctuations in x and y appear to be only weakly correlated.

As the velocity fluctuations are due to the crowding of the surrounding particles, the fluctuations may become more severe as the glass transition is approached. However, this is not the case, as is seen in Fig. 4 which shows the standard deviation of the instantaneous velocity σ_{v_x} plotted against the average velocity \bar{v} . Different symbols indicate different volume fractions, yet what is seen is that it is not the volume fraction which determines the standard deviation but the average velocity. The bigger the velocity of the magnetic bead the greater fluctuations of the velocity. Denser suspensions have slower velocities for the same force (as seen in Fig. 1) but also correspondingly smaller velocity fluctuations. The data are more scattered at low velocities and for any given sample the data scatter on both sides of the fit line. A similar trend holds for the transverse fluctuations, and

we find in general that $\sigma_{vy} = 0.4\sigma_{vx}$.

There are several possible origins of these velocity fluctuations. One possibility is that the applied force itself can cause the transient jamming of colloidal particles that are in front of the bead which break up due to Brownian motion [11]. Another possible cause of the intermittent motion of the magnetic bead might be intrinsic to the system. Dense colloidal suspensions are spatially heterogeneous systems [2, 3] and some regions may be “glassier” and thus harder to move through.

The changing character of the motion as the glass transition is approached can be understood by calculating the modified Peclet number. This is the ratio of two time scales, τ_B characterizing the unforced motion of the colloidal particles, and τ_M characterizing the motion of the magnetic bead. The Brownian time $\tau_B = a^2/2D_\infty$ is the time it takes for colloidal particles to diffuse a distance equal to their radius a and is based on their asymptotic diffusion constant D_∞ . D_∞ becomes small close to the glass transition, due to the crowding of the particles, and becomes zero for a colloidal glass. The magnetic bead time scale $\tau_M = a/\bar{v}$ is the time scale for the magnetic bead to move the distance a and is based on the magnetic bead’s average velocity \bar{v} . The modified Peclet number is then $Pe^* = \tau_B/\tau_M$ and is larger than 1 for all open symbols shown in Fig. 1 [12]. For the largest forces, $Pe^* \approx 10000$. Therefore, the forced motion of the magnetic bead is much more significant than the Brownian motion of the surrounding colloidal particles: the magnetic bead pushes these particles out of the way, plastically rearranging the sample. This results in an apparent lowering of the effective viscosity acting on the magnetic bead at higher velocities. On the macroscopic scale, this may correspond to traditional rheological measurements at high strains. Previous work found for similar colloidal samples that the viscoelastic moduli decreased as the maximum strain increased [13].

Since $Pe^* > 1$, the Brownian motion should be unimportant, similar to a granular system. Moreover, conjectures of the existence of a “jamming transition” speculate that the colloidal glass transition is similar to jamming in granular media [11, 14], and so it is interesting to compare our results with studies performed in a granular media. Albert *et al.* immersed a cylinder in granular particles and measured the force exerted on the cylinder when it moved with constant speed relative to the particles [15]. They found that the drag force on the cylinder is independent of the velocity, quite different from our behavior (Fig. 1). In our experiments, the solvent viscosity or Brownian motion (despite the high value of Pe^*) may be important, causing a velocity dependent drag force.

In conclusion, we find that near the glass transition the motion of a microsphere through a colloidal suspension changes dramatically. A threshold force appears, below which the sphere does not move, and this threshold force increases as the glass transition is approached. The ex-

istence of the threshold force hints that the system may locally “jam” even when the colloidal suspension is globally unjammed (not glassy). Above this threshold force the velocity is related to the force by a power law and the sphere moves with a fluctuating velocity locally deforming the sample. At high forces, the velocity is related to the force by a power law. This can be inverted to obtain an effective drag force on the sphere, growing weakly with velocity, $F \sim v^{1/\alpha}$ with α growing from 1 far from the glass transition to above 3 close to the transition. These results indicate that the onset of the glass transition in the colloidal suspension is signaled by a growing nonlinearity of the drag force. Our findings present a useful test of glass transition theories, as well as a new way to characterize the glass transition in colloidal suspensions.

We thank R. E. Courtland, M. B. Hastings, S. A. Koehler, D. Nelson, T. Squires, T. A. Witten, and S. Wu for helpful discussions. We thank A. Schofield for providing our colloidal samples. This work was supported by NASA (NAG3-2284).

-
- [*] Email: phabdas@physics.emory.edu
 [†] Current address: Department of Physics, University of Toronto, Toronto M5S 1A7, Ontario, Canada
 [‡] Email: weeks@physics.emory.edu
 [1] M. D. Ediger, C. A. Angell, S. R. Nagel, *J. Phys. Chem.* **100**, 13200 (1996); C. A. Angell, *J. Phys. Cond. Mat.* **12**, 6463 (2000).
 [2] W. K. Kegel and A. van Blaaderen, *Science* **287**, 290 (2000).
 [3] E. R. Weeks, J. C. Crocker, A. C. Levitt, A. Schofield, D. A. Weitz, *Science* **287**, 627 (2000).
 [4] E. R. Weeks and D. A. Weitz, *Phys. Rev. Lett.* **89**, 095704 (2002); E. R. Weeks and D. A. Weitz, *Chem. Phys.* **284**, 361 (2002).
 [5] A. Kasper, E. Bartsch, H. Sillescu, *Langmuir* **14**, 5004 (1998); A. H. Marcus, J. Schofield, S. A. Rice, *Phys. Rev. E* **60**, 5736 (1999).
 [6] I. M. Krieger, *Adv. Colloid Interface Sci.* **3**, 111 (1972); P. N. Segre, S. P. Meeker, P. N. Pusey, and W. C. K. Poon, *Phys. Rev. Lett.* **75**, 958 (1995).
 [7] Z. Cheng, J. Zhu, P. M. Chaikin, S-E Phan, and W.B. Russel, *Phys. Rev. E* **65**, 041405-1 (2002).
 [8] J. C. Crocker and D. G. Grier, *J. Colloid Interface Sci.* **179**, 298 (1996).
 [9] M.B. Hastings, C.J. Olson Reichhardt, C. Reichhardt, *Phys. Rev. Lett.* **90**, 098302-1 (2003).
 [10] R. E. Courtland and E. R. Weeks, *J. Phys. Cond. Mat.* **15**, S359 (2003).
 [11] M. E. Cates, J. P. Wittmer, J.-P. Bouchaud, and P. Claudin, *Chaos* **9**, 511 (1999).
 [12] We term this the “modified” Peclet number as we are using D_∞ rather than D_0 , the diffusion constant characterizing particle motion in dilute samples.
 [13] T. G. Mason and D. A. Weitz, *Phys. Rev. Lett.* **75**, 2770 (1995).
 [14] A. J. Liu and S. R. Nagel, *Nature* **396**, 21 (1998).
 [15] R. Albert, M. A. Pfeifer, A.-L. Barabasi, and P. Schiffer,

Phys. Rev. Lett. **82**, 205 (1999).